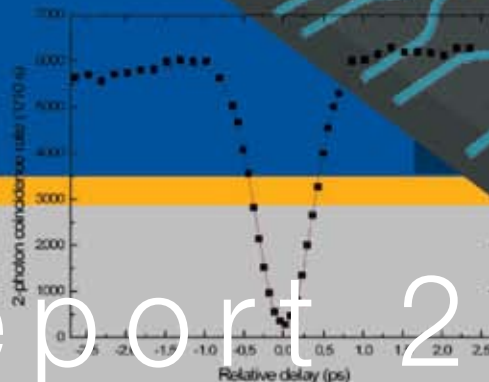
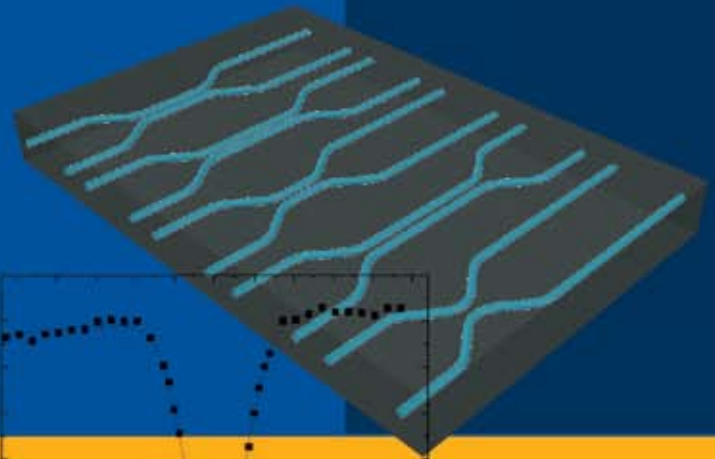
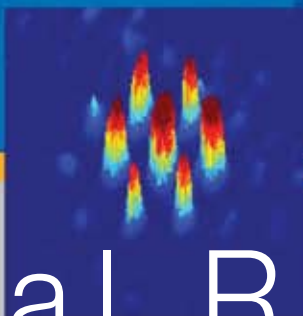
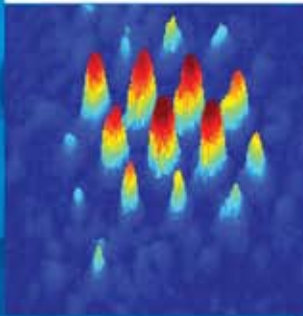
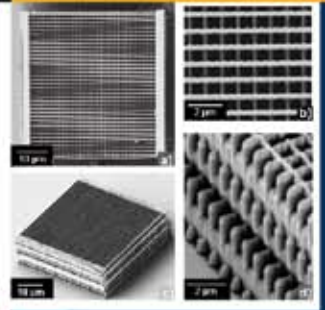
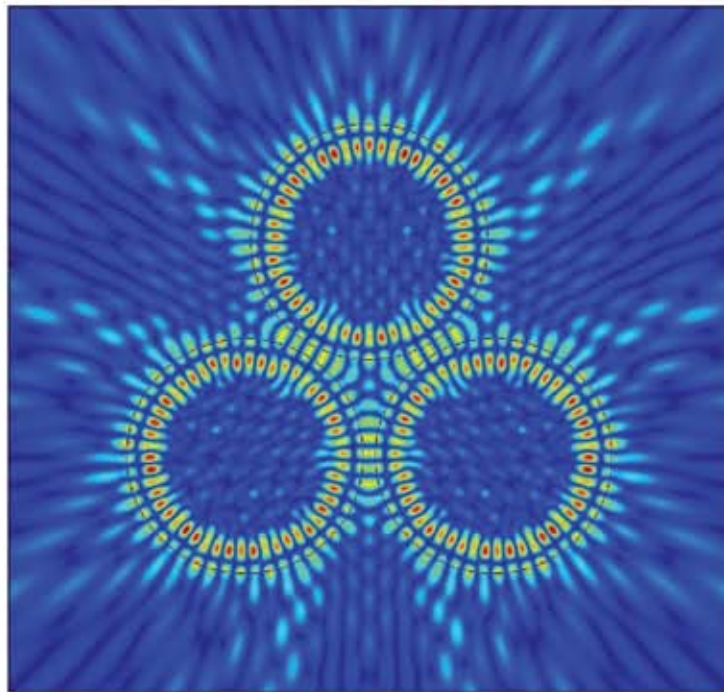
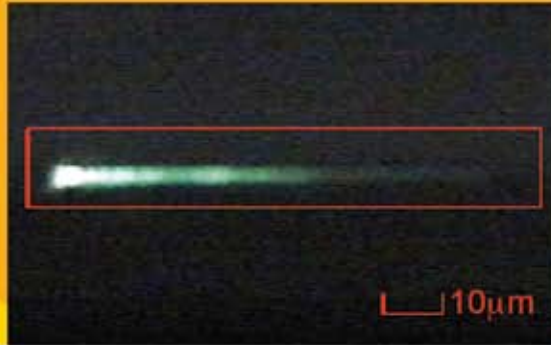


# CUDOS

The Centre for Ultrahigh bandwidth Devices for Optical Systems (CUDOS)



Annual Report 2008

# Chief Investigator: Barry Luther-Davies



## CI short biography

Barry Luther-Davies is a Professor of Laser Physics at the Australian National University with 38 years research experience in the diverse areas such as lasers, laser-matter interaction physics, photonics, optical materials and nonlinear optics. He completed a BSc in Electronics and PhD in Laser Physics from the University of Southampton, UK.

Barry oversees the Centre's work at ANU fabricating planar optical waveguide devices and photonic crystals in chalcogenide glasses and is also science leader of the CUDOS flagship project Compact Optical Switch in 2-D Photonic Crystal which combines the skills of researchers at ANU, The University of Sydney and the University of Technology Sydney. His broad experience contributes to all aspects of the CUDOS projects that spans materials science; film deposition and patterning; optical characterization; and device design.

Barry is an elected Fellow of the Optical Society of America and the Australian Academy for Technological Sciences and Engineering. He was awarded the Pawsey Medal of the Australian Academy of Science in 1986 for his contribution to laser-plasma interaction physics. He is currently a topical editor for the Journal of the Optical Society of America-B and an Advisory Editor for Optics Communications.

## Key areas of research contribution within the Centre

### Roles and responsibilities within Centre:

Group Leader: Laser Physics Centre, RSPHysSE, ANU;

Science Leader: *Compact Optical Switch in 2-D Photonic Crystal*.

### Describe key areas of research activity

Barry Luther-Davies oversees research into properties of new chalcogenide glasses; thin chalcogenide film production by pulsed laser ablation; film processing for waveguide and photonic crystals; device and materials testing. Devices are supplied to the flagship projects Integrated Chalcogenide Glass All-optical Regenerator and Compact Optical Switch in a 2-D Photonic Crystal.

## Research Achievements

### Nonlinear Materials and Planar Structures

#### Team:

Barry Luther-Davies  
Duk-yong Choi  
Steve Madden  
Rongping Wang  
Andrei Rode  
Douglas Bulla  
Maryla Krolikowska  
Anita Smith  
Darren Freeman  
Amrita Prasad  
Xin Gai  
Ting Han

### Overview

Our program underpins CUDOS-wide efforts to demonstrate high performance all-optical processors exploiting the third order nonlinearity of chalcogenide glasses. Our research includes the fabrication of novel glasses; studies of their basic physical and optical properties; film production and characterization; and film processing to create low loss optical waveguides and photonic crystals. Structures are supplied to the flagship projects "Chalcogenide Integrated Circuits" and "Compact Optical Switch".

### Bulk chalcogenide glasses and their properties

Chalcogenide glasses comprise a wide range of amorphous materials containing the chalcogen elements S, Se and Te compounded with network forming elements such as As, Ge, Si, etc. We have chosen these materials for our photonic devices because they have high refractive index, large third order nonlinearity, and photosensitivity whilst being free of absorption across the whole of the near- and mid-infra-red. A challenge with chalcogenides arises from their relatively weak chemical bonding which results in low melting temperatures and structural instability. These lead to a range of exotic phenomena such as quasi-crystallization and enhanced photosensitivity even at wavelengths well beyond their band edge.

We have continued to study the properties of chalcogenide bulk glasses and films, in particular, to identify the most stable compositions with high optical nonlinearity suitable for photonics applications. Our fundamental studies focussed on understanding the structure of bulk glasses using x-ray photoelectron spectroscopy (XPS) were continued this year in collaboration with the group of Professor Himanshu Jain at Lehigh University in the USA. Rongping Wang visited Professor Jain's laboratory in April supported by funding from the Australian Academy of Sciences and Lehigh University to use their high-resolution XPS facility to study the chemical order in Ge-As-Se glasses. The results of these studies revealed a clear evolution of the chemical bonds in the glass as a function of mean coordination number (MCN – the sum of the product of the valency times the atomic fraction of the constituent elements). It has been widely discussed that the MCN determines the basic topology of the Ge-As-Se glass network with transitions from a "floppy" to stress-free rigid network occurring at  $MCN \approx 2.4$ ; whilst a second transition to a stressed-rigid 3-D network is expected at  $MCN \approx 2.67$ . These limits also correspond the boundaries outside which the glasses in the ternary Ge-As-Se system can no longer

be stoichiometric. Hence defect or wrong bonds must exist in the glasses for  $MCN > 2.67$  or  $< 2.4$ . Last year we identified rapidly increasing optical losses in high MCN glasses which appeared to correlate with features in Raman spectra we associated with Ge-Ge or As-As defect bonds.

The high resolution XPS spectra obtained at Lehigh confirmed this interpretation and have allowed us to quantify how the various chemical bonds in the glasses evolve with MCN. Some results are shown in Fig. 1 where we have plotted the relative abundance of different bonds with increasing MCN. It is quite apparent that at low MCN, the glass structure is dominated by the existence of ideal Arsenic pyramidal and Germanium tetrahedral structures but also contain a significant fraction of Se trimers. At high MCN, however, the Se trimers disappear completely as do the perfect pyramidal and tetrahedral structures and are replaced by units containing wrong bonds such as As-As-2Se and 2Ge-Ge-2Se. Of the samples studied, that with  $MCN = 2.5$  corresponded to a chemically stoichiometric glass. It is clear from this picture that above  $MCN = 2.55$  the number of wrong or defect bonds in the glass increases rapidly. This results in a rapid increase in the optical losses of the glass because these defect bonds create states in the band gap that result in an exponentially decaying absorption tail extending into the infra-red. As a result high MCN glasses are not well-suited to photonic applications at 1550 nm.

In other studies of fundamental glass properties we have measured the densities, refractive index and elastic properties of glasses in the Ge-As-Se system to search for signatures of the change in network topology predicted for this ternary glass system as a function of MCN. The elastic properties of glass samples were determined from the shear and compressive wave velocities measured by ultrasonic pulse interferometry in collaboration with the group of Professor Ian Jackson at the Research School of Earth Sciences at ANU. The material densities are required to determine the elastic moduli but can affect optical properties such as the index of refraction.

Figure 2 shows the material density for 17 glasses in the Ge-As-Se system along with data for similar glasses from the literature. It is apparent that there is a maximum in density for MCN around 2.4 and a minimum at MCN around 2.7. The scatter is large most likely because MCN may not be the most appropriate abscissa in this case. For example, the same MCN can be obtained for different glasses with quite different chemical compositions, some of which may lie in regions of the phase diagram where nanophase separation occurs, others of which may be closer or further from a chemically stoichiometric mixture and, therefore, contain different numbers of wrong or defect bonds. We have evidence from our data that such factors may well have a marked effect on density. Fig. 4 shows data for the refractive index of the bulk glass as a function of MCN. These data dramatically reflect the different structural regions predicted for these glasses and also correlate with the measured variation in glass density. Whilst there is considerable complexity involved in relating material density to index of refraction, such a correlation is reasonable for glasses composed of the same elements if the polarizability changes only weakly with composition.

The results for the elastic moduli are shown in figure 3(a) and (b) for shear and compression waves respectively. We have identified for the first time the existence of two transitions for the elastic moduli again corresponded to the expected transitions from the

floppy to intermediate and from the intermediate to stressed-rigid phases. Taken overall these data provide very strong support for the models of Philips<sup>1</sup>, Thorpe<sup>2</sup>, Boolchand<sup>3</sup> and Tanaka<sup>4</sup>.

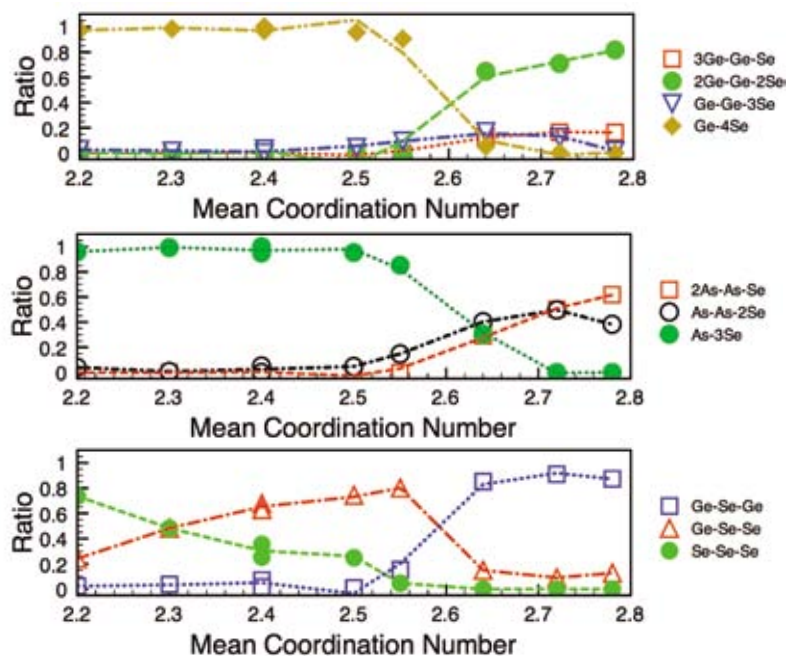


Fig 1. The relative abundance of different bonds in Ge-As-Se glasses as a function of MCN.

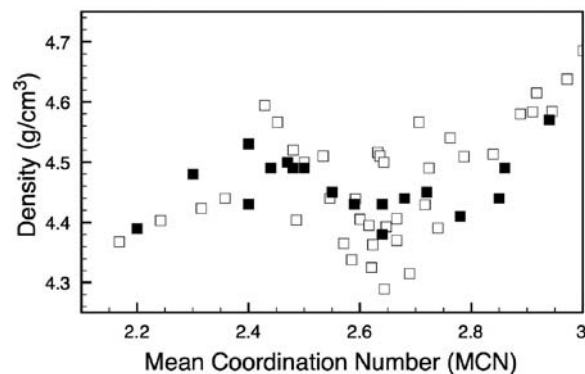
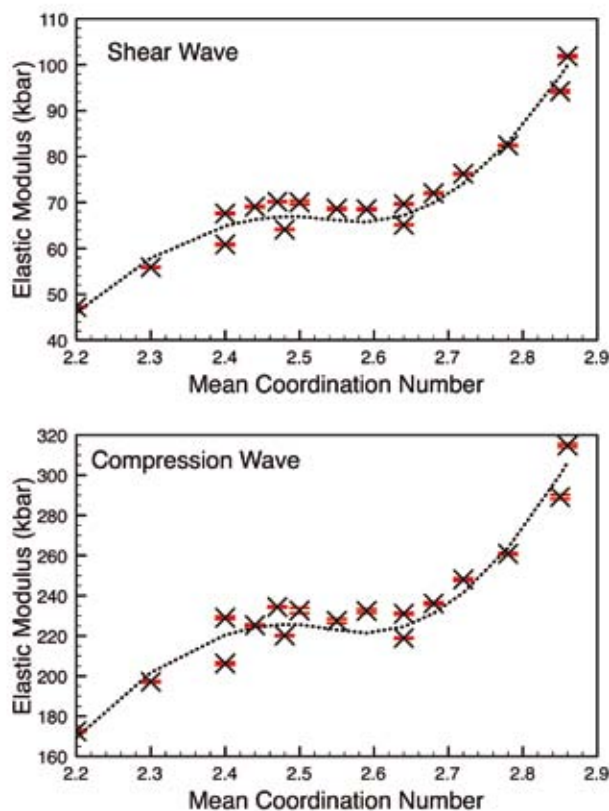


Fig 2. Density of Ge-As-Se glasses as a function of MCN.



**Fig 3. (a) LHS: Shear wave elastic modulus for Ge-As-Se glasses as a function of MCN; and (b) RHS Compression wave elastic modulus as a function of MCN.**

### Relevant Publications and Presentations

1. Wang, R. P., A. V. Rode, D. Y. Choi and B. Luther-Davies (2008). Investigation of the structure of  $\text{Ge}_x\text{As}_y\text{Se}_{1-x-y}$  glasses by x-ray photoelectron spectroscopy. *Journal of Applied Physics* 103(8).
2. Wang, R. P., A. Rode, D. Y. Choi and B. Luther-Davies (2008). Surface oxidation of  $\text{Ge}_{33}\text{As}_{12}\text{Se}_{55}$  films. *Journal of the American Ceramic Society* 91(7): 2371-2373.
3. Prasad, A., C. J. Zha, R. P. Wang, A. Smith, S. Madden and B. Luther-Davies (2008). Properties of  $\text{Ge}_x\text{As}_y\text{Se}_{1-x-y}$  glasses for all-optical signal processing. *Optics Express* 16(4): 2804-2815.
4. R.P. Wang, D.Y. Choi, A.V. Rode, B. Luther-Davies, "The Evolution of bond structure in  $\text{Ge}_{33}\text{As}_{12}\text{Se}_{55}$  films upon thermal annealing", 9th International Workshop on Non-crystalline Solids, 27-30 April 2008, Porto, Portugal
5. R.P. Wang, A. Smith, B. Luther-Davies, "Microstructure of  $\text{Ge}_x\text{As}_y\text{Se}_{1-x-y}$  Glasses", IUMRS-ICEM 2008, 28th July - 1st August 2008, Sydney, Australia
6. R.P. Wang, A. Smith, B. Luther-Davies, "Raman spectra of  $\text{Ge}_x\text{As}_y\text{Se}_{1-x-y}$  glasses", Unifying Concepts in Glass Physics IV, November 25-28, 2008 Kyoto, Japan

### Film properties and processing

Last year we reported that thermal evaporation could be used to prepare films of Ge-As-Se glasses with similar stoichiometry to the bulk glasses provided the evaporation rate of the material was carefully controlled via the boat temperature. We also obtained the first evidence that some glass compositions could be deposited as thin films with physical properties such as their index of refraction very close to the bulk values and that the film index was insensitive to annealing up to the glass transition temperature. During 2008 we extended these studies to a wider range of films finding a narrow range of glass compositions overlapping with the so-called intermediate phase that could be deposited with the same index as the bulk. Outside this region corresponding to MCN between 2.4 and 2.55, the index of the films was substantially larger than that of the parent glass. This is illustrated in Figure 4, where the index of as-deposited films is compared with those of the bulk glass as a function of MCN. Similar behaviour can be seen in Fig. 5 which plots values of the optical gap (obtained in this case from the model fit from our SCI FilmTek 4000 wafer mapper used to measure film refractive indices). In the range of MCN between 2.4 and 2.55 the optical gaps of as-deposited films and bulk glass (obtained from a conventional Tauc plot obtained from the transmission spectrum of bulk glass samples 10-20 $\mu\text{m}$  thick) were the same within the experimental error. However, outside this region the optical gap of the as-deposited films was substantially reduced relative to the bulk glasses.

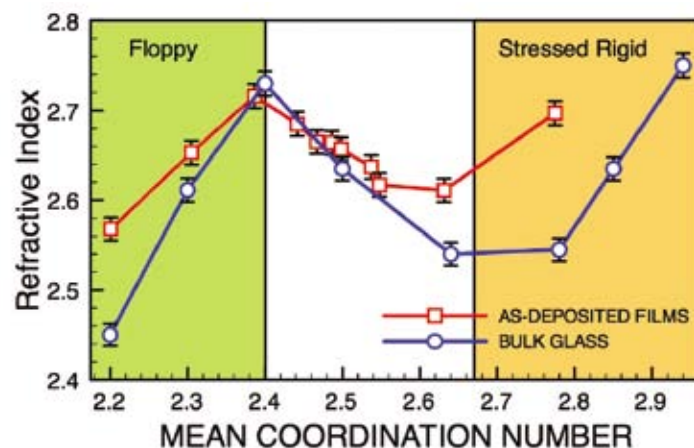


**Fig 4. Variation of refractive index of as-deposited films compared with bulk glasses.**

Upon annealing at temperatures up to  $T_g$ , the properties of glasses (refractive index and optical gap) with high MCN ( $>2.6$ ) evolved steadily towards their bulk glass values. This is consistent with our previous results reported for  $\text{Ge}_{33}\text{As}_{12}\text{Se}_{55}$ . XPS data indicate that for these glasses the bond structure of the as-deposited films differs significantly from that of the bulk glass. Upon annealing, however, the bonds rearrange trending towards those characteristic of the bulk. However this process is generally accompanied by changes in glass density (expansion in the case of high MCN glasses) which results in the films becoming stressed, which can result in cracking or delamination if such films are processed into optical waveguides.

For low MCN films (<2.3), annealing produces no changes in index or optical gap. It must be remembered, however that for these materials  $T_g$  is low (<150 C) and hence the maximum annealing temperatures are limited compared with the high MCN glasses where  $T_g > 300$  C. We conclude here that these films deposit in an amorphous state with chemical bonds different from that of the bulk glass. The activation energy is too high for the bonds to rearrange at temperatures less than 150 C. Thus these films remain trapped in an amorphous state different from the glass state.

For samples in the intermediate range of MCN (2.4-2.55) annealing has a negligible effect on refractive index whilst a small increase in optical gap could be detected. This is consistent with the work of Mott and Davies where annealing is expected to generally improve the network topology particularly reducing the number of defects and this is predicted to result in a blue shift in the optical gap. XPS studies of these intermediate MCN films showed that their bond structure is indistinguishable from that of the bulk glass and is not changed by annealing. Thus we conclude that in this particular range of MCN, as-deposited films form directly into the glass state in spite of the non-equilibrium conditions in which they are created. Nevertheless the as-deposited network contains defects that can be eliminated by annealing. The implication is that for this small range of MCN, the glass state which represents the global minimum of the potential energy of the network, is not separated by significant potential barriers from other amorphous states. On the other hand, for high (or low) MCN glasses the as-deposited films become trapped in an amorphous state separated from that of the glass by a significant energy barrier. In the case of high MCN glasses annealing around 300 C provides sufficient energy for the network to cross this barrier thereby relaxing towards the glass.

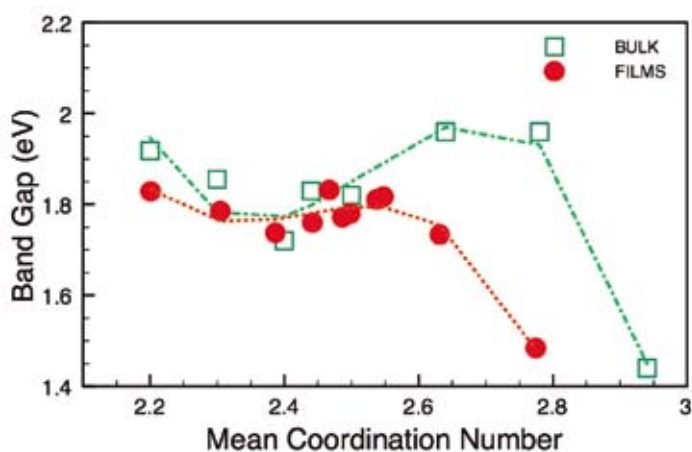


**Fig 5. Optical gap of as-deposited films compared with values for the bulk glass.**

### Nanostructure of $As_2S_3$ thermally deposited thin films

When we fabricate  $As_2S_3$  waveguides for all-optical processing using lithography and plasma etching, we have found that the etched surfaces often become roughened on the nanometre scale, something we have speculated as due to selective etching of nanoscale heterogeneity present in the thermally evaporated glasses. Such a process will ultimately limit the minimum losses than can be obtained in chalcogenide waveguides and particularly photonic nanowires required to obtain ultra-high nonlinear response.

To examine the existence of nanoscale heterogeneity in thermally evaporated  $As_2S_3$  films we have employed high resolution TEM and fluctuation electron microscopy (FEM) in collaboration with Dr Amelia Liu from Monash University and Dr Xidong Chen from the Argonne National Laboratory in the USA.

FEM is a technique capable of revealing medium range order in the films on the scale of 1-3nm. We used the tilted dark field technique which is a way of statistically sampling scattering from different regions in the material. If there is a large difference between the scattering from adjacent regions, then the material contains regions of correlated structure. The method is not fully quantitative but allows a comparison between materials with similar composition and density. In this work, therefore, we chose to compare as-deposited films with those that had been subjected to thermal annealing at 130C for 24h. FEM signals for these two films are shown in Fig. 6.

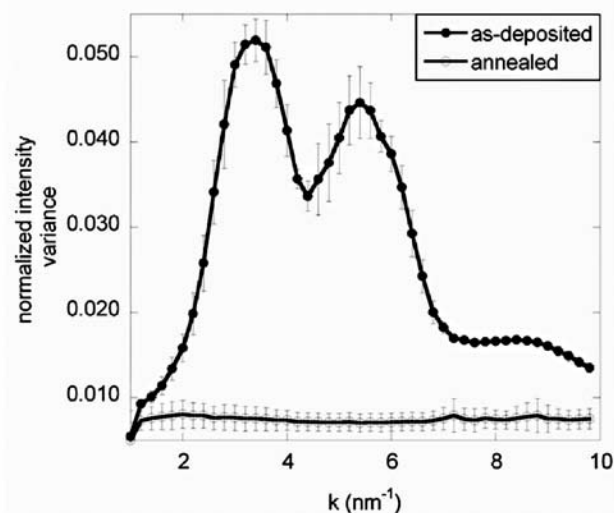


**Fig 6. FEM data from as-deposited and annealed  $As_2S_3$  films. The normalised variance gives a measure of the heterogeneity in the films. Clearly the annealed films has substantially reduced heterogeneity than the as-deposited one.**

It is apparent from Fig. 6 that the variance in the as-deposited samples is large compared with those that have undergone thermal annealing. Thus as-deposited films contain quasi-stoichiometric structurally correlated regions with granular interfaces. The high degree of medium range order in the as-deposited films means that the as-deposited structure represents a maximum in the energy landscape. Thermal annealing reduces the overall free energy by dissolving regions of correlated structure creating a more continuous glass network. This graphically illustrates why thermal annealing is essential to reducing optical losses in  $As_2S_3$  waveguides.

A number of other observations emerged from these studies. HRTEM revealed that both as-deposited and annealed samples contained nano-crystallites (see figure 7). These were observable as regions containing lattice fringes about 10 nm in extent. Interestingly upon annealing a significant change in lattice spacing could be observed consistent with a change from realgar ( $AsS$ ) to orpiment ( $As_2S_3$ ) crystalline phases. These nano-crystallites, however, comprise a relatively small volume of the material and diffraction patterns

from an areal average of 200 nm diameter resulted in diffuse rings characteristic of the amorphous state. Nevertheless the presence of such crystallites may ultimately affect the smoothness of etched sidewalls that can be obtained in these materials.

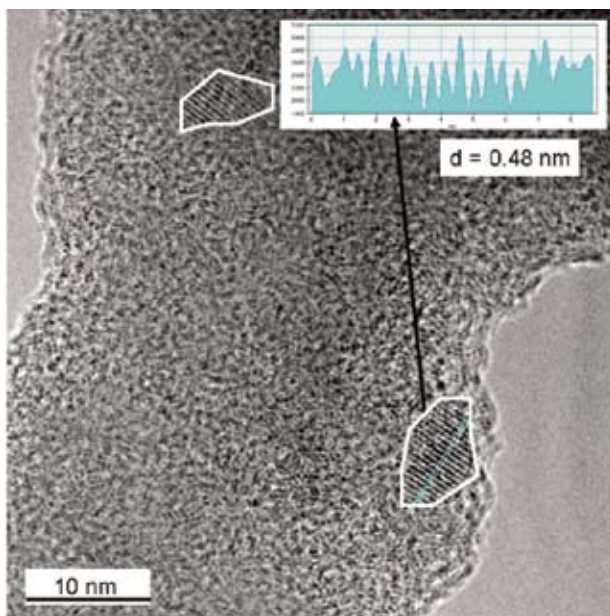


**Fig 7. HRTEM image of an annealed  $\text{As}_2\text{S}_3$  film showing 1nm x 5nm crystallites with a lattice fringe spacing of 0.48nm.**

### Relevant Publications and Presentations

- Liu, A. C. Y., X. Chen, D. Y. Choi and B. Luther-Davies (2008). Annealing-induced reduction in nanoscale heterogeneity of thermally evaporated amorphous  $\text{As}_2\text{S}_3$  films. *Journal of Applied Physics* 104(9).
- Duk-Yong Choi, Amelia Liu, Steve Madden, Andrei Rode, Rongping Wang, Douglas Bulla, Barry Luther-Davies "The effect of heat treatment on the microstructure of thermally evaporated  $\text{As}_2\text{S}_3$  film," Spring MRS 2008, San Francisco, 24-28 March (2008).

### Device fabrication

This year our fabrication efforts concentrated on producing waveguides with enhanced nonlinearity in  $\text{As}_2\text{S}_3$  with mode area reduced both to increase the nonlinear response but more importantly to access the region of zero or anomalous dispersion. Modelling results suggested that rib waveguides fabricated in films around 850 nm thick would display anomalous dispersion at 1550 nm for rib widths in the 2-3  $\mu\text{m}$  range corresponding to mode volumes in the 1-2  $\mu\text{m}^2$  range and nonlinear parameters of 5000-10000  $\text{W}^{-1}\text{km}^{-1}$ . Reducing mode volume, however, results in stronger interaction between the fields and waveguide walls making the optical losses more sensitive to surface roughness or absorption. As a result we have had to continue work on process optimisation aimed at reducing losses in these waveguides.

To date our best results have been obtained in 4  $\mu\text{m}$  wide waveguides in 0.85  $\mu\text{m}$  thick films where we observe losses about 0.25 dB/cm, whilst in waveguides with a higher nonlinear response (2  $\mu\text{m}$  wide in 0.85  $\mu\text{m}$  films (Figure 8) of  $\gamma=10,000\text{W}^{-1}\text{km}^{-1}$  the losses increased to 0.5 dB/cm at best. These higher losses have in part been found to problems with the protective layer required

to protect the  $\text{As}_2\text{S}_3$  from attack by photoresist developer. In our most recent process we have employed BARC as the protective layer, however, during the BARC stripping process has been found to increase optical losses. As a result PMMA/BARC composites or SU8 films are now being used as protective layers as a route to reducing losses further.

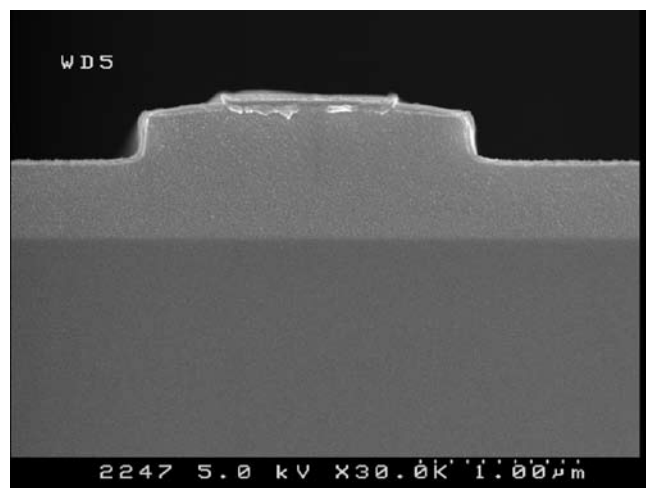


**Fig 8. Cross section of 0.85 $\mu\text{m}$  x 2 $\mu\text{m}$  rib waveguide with anomalous dispersion at 1550nm.**

Our work on  $\text{Ge}_{11}\text{As}_{22}\text{Se}_{67}$  glass has continued and we are attempting to fabricate nano-wires with very large  $\gamma$  ( $>40,000\text{W}^{-1}\text{km}^{-1}$ ) and anomalous dispersion. For this particular material it has proven to be impossible to engineer anomalous dispersion at 1550 nm in IPG coated rib waveguides whilst uncoated ribs only a small parameter space exists when anomalous dispersion can be obtained.

Using  $\text{As}_2\text{S}_3$  waveguides displaying anomalous dispersion a number of exciting results have been obtained some of which are reported elsewhere. These have included low threshold supercontinuum generation; four wave mixing gain; and recently Raman amplification. The results of a recent experiment demonstrating Raman gain are shown in Figure 9. In this case a weak ( $<100\mu\text{W}$ ) TM polarised tuneable CW probe beam was co-propagated with  $\approx 4$  ps duration 20 W peak power pump pulses at 1555 nm through a 40 cm long, 0.85  $\mu\text{m}$  x 4  $\mu\text{m}$   $\text{As}_2\text{S}_3$  waveguide. Fig. 9 shows the output spectrum for two different cases: probe injected at 1615nm; and probe injected at 1640 nm. In the first case the probe corresponds to the wavelength where FWM dominates the nonlinear process. Thus the probe is amplified and at the same time an equal amplitude "idler" is generated at 1499 nm with roughly the same power as in the amplified probe. When the probe is tuned to 1640 nm, however, which corresponds to overlap with the peak of the Raman gain, the spectrum is asymmetric with the signal at 1478 nm being -30 dB relative to that at 1640 nm. Maximum FWM gain occurred at 1590 nm in this waveguide as indicated by the peak in the spectra due to amplification of ASE background from the pump laser.

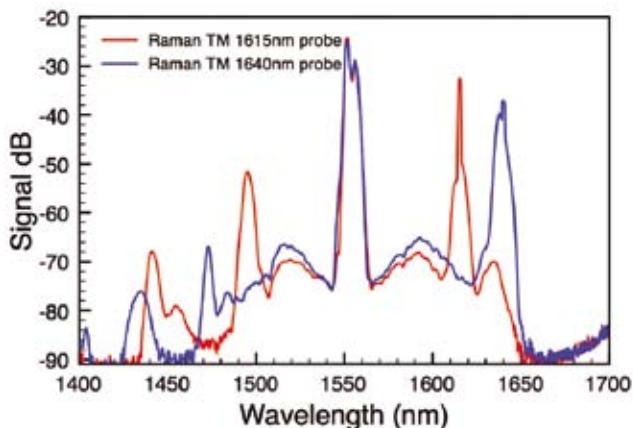


**Fig 9. Output spectra from a 40cm long  $\text{As}_2\text{S}_3$  waveguide when co-propagating a 20W 1555nm pump laser pulses with a co-propagating tuneable CW probe. With the probe tuned to 1640nm, amplification occurs due to Raman gain, whilst at 1615nm, four wave mixing dominates.**

### Relevant Publications and Presentations

9. Choi, D. Y., S. Madden, A. Rode, R. P. Wang, A. Ankiewicz and B. Luther-Davies (2008). Surface roughness in plasma-etched  $\text{As}_2\text{S}_3$  films: Its origin and improvement. *IEEE Transactions on Nanotechnology* 7(3): 285-290.
10. Lamont, M. R. E., B. Luther-Davies, D. Y. Choi, S. Madden, X. Gai and B. J. Eggleton (2008). Net-gain from a parametric amplifier on a chalcogenide optical chip. *Optics Express* 16(25): 20374-20381.
11. Choi, D. Y., S. Maden, A. Rode, R. P. Wang and B. Luther-Davies (2008). Plasma etching of  $\text{As}_2\text{S}_3$  films for optical waveguides. *Journal of Non-Crystalline Solids* 354(27): 3179-3183.
12. Pelusi, M. D., V. G. Ta'eed, L. B. Fu, E. Magi, M. R. E. Lamont, S. Madden, D. Y. Choi, D. A. P. Bulla, B. Luther-Davies and B. J. Eggleton (2008). Applications of highly-nonlinear chalcogenide glass devices tailored for high-speed all-optical signal processing. *IEEE Journal of Selected Topics in Quantum Electronics* 14(3): 529-539.
13. Lamont, M. R. E., B. Luther-Davies, D. Y. Choi, S. Madden and B. J. Eggleton (2008). Supercontinuum generation in dispersion engineered highly nonlinear ( $\gamma=10/\text{W/m}$ )  $\text{As}_2\text{S}_3$  chalcogenide planar waveguide. *Optics Express* 16(19): 14938-14944.
14. Duk-Yong Choi, Steve Madden, Andrei Rode, Rongping Wang, Douglas Bulla, Barry Luther-Davies, "CHF<sub>3</sub> Gas Flow Rate Effect on the Plasma Etching Characteristics of  $\text{As}_2\text{S}_3$  Films," *ICONN 2008*, Melbourne, 25-29 Feb (2008)
15. Duk-Yong Choi, Steve Madden, Andrei Rode, Rongping Wang, Barry Luther-Davies "Dry etching of amorphous  $\text{As}_2\text{S}_3$  films in CHF<sub>3</sub> plasma," *UMRS-ICEM2008*, Sydney, 28 Jul – 1 Aug (2008)
16. Duk-Yong Choi, Barry Luther-Davies "All-optical signal processors using chalcogenide glasses: the materials preparation, properties, and processing," *The Korean institute of Metals and Materials*, Incheon (Korea), 23-24 Oct (2008)
17. Duk-Yong Choi, Steve Madden, Andrei Rode, Rongping Wang, Barry Luther-Davies "Dry etching characteristics

of amorphous  $\text{As}_2\text{S}_3$  film in CHF<sub>3</sub> plasma," *Australian Institute of Physics 18th National Congress*, Adelaide, 30 Nov – 5 Dec

18. DukYong Choi, Steve Madden, Andrei Rode, Rongping Wang, Douglas Bulla, Barry Luther-Davies, "A protective layer on  $\text{As}_2\text{S}_3$  film for photo-resist patterning," *Ninth International Workshop on Non-Crystalline Solids*, 27-30 April 2008, Porto, Portugal.
19. Ta'eed, V. G., M. D. Pelusi, B. J. Eggleton, D. Y. Choi, S. Madden, D. A. P. Bulla and B. Luther-Davies (2008). All-optical wavelength conversion of 80 Gb/s signal in highly nonlinear serpentine chalcogenide planar waveguides. *2008 Conference on Optical Fiber Communication/National Fiber Optic Engineers Conference*, Vols 1-8: 1449-1451.
20. Pelusi, M. D., V. G. Ta'eed, M. R. E. Lamont, B. J. Eggleton, S. Madden, D. Y. Choi, D. A. P. Bulla and B. Luther-Davies (2008). Optical signal processing in highly-nonlinear chalcogenide planar waveguides. *2008 IEEE/LEOS Winter Topical Meeting Series*: 86-87.
21. Luther-Davies, B., D. Y. Choi, A. Prasad, R. Wang, D. Bulla, C. Zha, M. Pelusi, V. Ta'eed, M. R. E. Lamont, L. Fu, D. J. Moss, K. Finsterbusch, H. C. Nguyen and B. J. Eggleton (2008). Nonlinear materials for integrated ultra-fast all-optical devices. *2008 IEEE/LEOS Winter Topical Meeting Series*: 2-3.
22. Baker, N. J., M. Roelens, S. Madden, B. Luther-Davies, C. M. de Sterke and B. J. Eggleton (2008). Modulation-instability and pulse-train generation in a highly nonlinear Bragg grating. *2008 IEEE/LEOS Winter Topical Meeting Series*: 35-36.
23. Baker, N. J., M. Roelens, S. Madden, B. Luther-Davies, C. M. de Sterke and B. J. Eggleton (2008). Modulation Instability & Bragg Soliton Formation in a Highly Nonlinear  $\text{As}_2\text{S}_3$  Waveguide Bragg Grating. *2008 Conference on Lasers and Electro-Optics & Quantum Electronics and Laser Science Conference*, Vols 1-9: 3564-3565.

### Photonic crystals

We have discontinued work on the production of 2-D photonic crystals by focussed ion beam milling changing to a more conventional approach based on e-beam lithography and dry etching following the installation of a new Raith 150 e-beam writer at ANU at the end of 2007. We have concentrated on developing processes for the production of photonic crystals in  $\text{Ge}_{33}\text{As}_{12}\text{Se}_{55}$  films deposited onto oxidised silicon wafers. These are aimed to be used to photo-define photonic crystal resonators in W1 waveguides by local exposure of the AMTIR-1 to 633nm light (reported elsewhere). This year we have concentrated on process development using PMMA as the photoresist and CHF<sub>3</sub> as the etchant. Following etching BOE was used to remove the silica layer creating a free-standing membrane. At present we have a successful and repeatable process (Fig. 10(a)) although there is room for improvement to eliminate residual roughness in the patterns and to eliminate bowing of the membranes after release (Fig. 10(b)). The latter is likely to be due to changes in the bond structure of the films, probably due to e-beam exposure, which as mentioned above are different from those of the bulk glass. In the case of AMTIR-1, relaxation of the bonds is known to result in a volume increase which is likely to result in the production of compressive stress in the films.

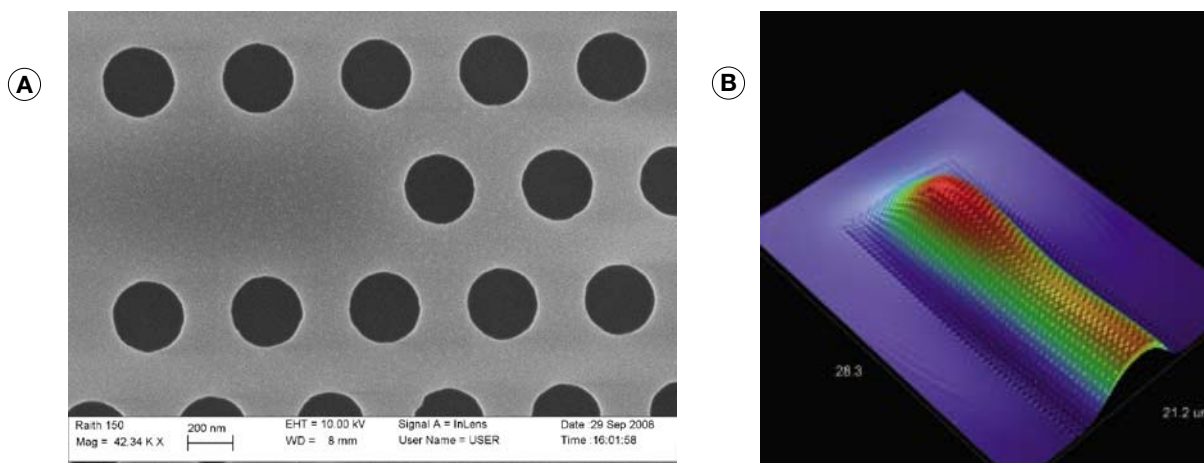


**Fig 10. (a): SEM image of part of an AMTIR-1 Photonic crystal fabricated by e-beam lithography at ANU. 10(b) Surface profile of the end of the membrane after removing the SiO<sub>2</sub> underlayer indicating that these membranes are under compressive stress and bow after release, most likely because of changes in bond structure of the glass as a result of e-beam irradiation.**

### Relevant Publications and Presentations

24. Lee, M. W., C. Grillet, C. G. Poulton, C. Monat, C. L. C. Smith, E. Magi, D. Freeman, S. Madden, B. Luther-Davies and B. J. Eggleton (2008). Characterizing photonic crystal waveguides with an expanded k-space evanescent coupling technique. *Optics Express* 16(18): 13800-13808.
25. Faraon, A., D. Englund, D. Bulla, B. Luther-Davies, B. J. Eggleton, N. Stoltz, P. Petroff and J. Vuckovic (2008). Local tuning of photonic crystal cavities using chalcogenide glasses. *Applied Physics Letters* 92(4).
26. Smith, C. L. C., D. K. C. Wu, M. W. Lee, C. Monat, S. Tomljenovic-Hanic, D. Freeman, S. Madden, C. Grillet, B. Luther-Davies, H. Giessen and B. J. Eggleton (2008). Microfluidic photonic crystal nanocavities - art. no. 680003. *Device and Process Technologies for Microelectronics, MEMS, Photonics and Nanotechnology IV* 6800: 80003-80003.
27. Karnutsch, C., C. L. C. Smith, D. K. C. Wu, S. Tomljenovic-Hanic, M. W. Lee, C. Monat, C. Grillet, R. McPhedran, B. J. Eggleton, D. Freeman, S. Madden and B. Luther-Davies (2008). Reconfigurable Microfluidic Photonic Crystal Cavities. *2008 Conference on Lasers and Electro-Optics & Quantum Electronics and Laser Science Conference*, Vols 1-9: 1027-1028.
28. Freeman, D., C. Grillet, M. W. Lee, C. L. C. Smith, Y. Ruan, A. Rode, M. Krolikowska, S. Tomljenovic-Hanic, C. M. De Sterke, M. J. Steel, B. Luther-Davies, S. Madden, D. J. Moss, Y. H. Lee and B. J. Eggleton (2008). Chalcogenide glass photonic crystals. *Photonics and Nanostructures-Fundamentals and Applications* 6(1): 3-11.
29. Faraon, A., D. Englund, D. Bulla, B. Luther-Davies, B. J. Eggleton, N. Stoltz, P. Petroff and J. Vuckovic (2008). Local tuning of photonic crystal cavities using chalcogenide glasses. *2008 Conference on Lasers and Electro-Optics & Quantum Electronics and Laser Science Conference*, Vols 1-9: 851-852.

### Facility Development

A number of facility upgrades were completed in 2008. These include improvements to and extension of our clean room to achieve better control of our processing environment. The ICP etching machine will be moved into the new clean room in early 2009.

A new optical profiler, funded by ANU, and capable of providing quantitative measurements of surface profiles has been installed for measuring roughness of etched surfaces, etch depths and device profiles. The system is a Veeco NT9100 and is capable of stitching profiles up to an area of 100x100mm with 0.4μm transverse spatial resolution and sub Å vertical resolution. An example of the capabilities of the instrument is shown in Fig. 10(b).